The Effect of the Ratio of Remanent Flux Density to Coercivity of Magnet on Spoke-Type Permanent Magnet Synchronous Motor (PMSM) Performance

Minyeong Choi¹, Yang-Ki Hong^{1,*}, Hoyun Won¹, Shuhui Li¹, S. Rahman¹, M. Nurunnabi¹, Woncheol Lee^{1,2}, and Chang-Dong Yeo³

¹Department of Electrical and Computer Engineering, Tuscaloosa, Alabama 35487, USA

²Samsung Electronics, Suwon, Gyeonggi-do 16677, South Korea

³Department of Mechanical Engineering, Texas Tech University, Lubbock, Texas 79409, USA

*Author to whom correspondence should be addressed: ykhong@eng.ua.edu

Abstract-- Spoke-type PMSMs were designed with commercial permanent magnets and theoretically designed hexaferrite: Nd-Fe-B (NdFe35, G1NH), Alnico (8B, 8H, 9), and La-CoSrM hexaferrite (NMF-15G). It was found that coercivity (H_c) plays a crucial role in determining motor performance. The ANSYS Maxwell software was used to characterize the designed motor performance. Commercial RE-free Alnico 9 holds a 10.5 MGOe of (BH)_{max}, much higher than a 5.5 MGOe of RE-free Alnico 8B/8H and SrM (SrFe₁₂O₁₉) hexaferrite magnets. However, the Alnico 9 motor performance is not better than the other Alnico 8B/8H and hexaferrite motors. The spoke-type PMSM with our theoretically designed SrM hexaferrite simulated motor performance. A motor performs best when the H_c/B_r ratio equals one with a high $\hat{H_c}$. For instance, the motor torque and peak power increase to 189 Nm and 178 kW, respectively, as the H_c increases to 4.86 kOe from 2.43 kOe. However, the motor performance is not significantly changed with a fixed H_c and various B_r . It was found that regardless of $(BH)_{max}$, coercivity (H_c) plays a dominant role in motor performance.

Index Terms—Spoke-type PMSM, Motor Performance, Magnetic Properties

I. INTRODUCTION

Electric Vehicles (EVs) are the future of most transportation. As the EV market grows, high-performance and rare-earth (RE) -free permanent magnets (PMs) have gained much interest due to their low cost and no-supply issue. However, RE-free permanent magnets hold a smaller maximum energy product (BH)_{max} than RE permanent magnets. To our best knowledge, the roles of coercivity in RE-free permanent magnet motor performance have not been reported. The automotive industry has adopted the interior permanent magnet synchronous motor (IPMSM) because of its high power density, high efficiency, and wide constant-power operating region. An electric motor with magnets arranged like spokes around the central hub offers superior torque, power density, and cooling capabilities in a smaller package than a standard IPMSM. Therefore, we have

chosen spoke-type PMSM to investigate the effects of the ratio of coercivity (H_c) to remanent magnetic flux density (B_r) of the RE-free permanent magnet on motor performance. We used the commercial permanent magnets and our theoretically developed RE-free permanent magnets in the motor performance evaluation.

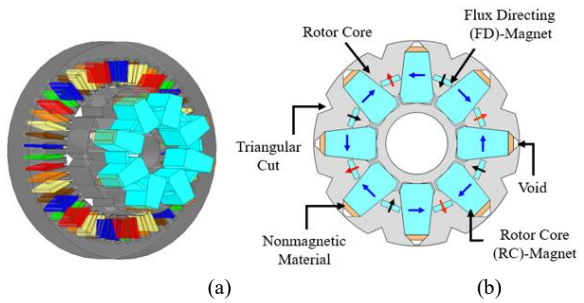


Fig. 1. Design of (a) 3D 6 phase spoke-type PMSM and (b) 2D rotor.

II. DESIGN OF SPOKE-TYPE PMSM

PMSM consists of the copper winding on the stator and permanent magnets on the rotor. There are four major components: rotor core (RC) magnet, flux directing (FD) magnet, nanomagnetic material, void, and triangular cut, as shown in Figure 1. Their roles are described below. The RC magnet enhances magnetic flux concentration, and the FD magnet help concentrate further in the middle and upper part of the rotor. The non-magnetic material suppresses the demagnetization irreversibly on the top of the RC magnet. The role of the void is to ensure a smooth flow of large weakening flux during flux-weakening operation. The triangular cut helps redirect and block the unnecessary winding flux. As described in the previous section, the PMSM has advantages such as high power density, small size, and high efficiency. Meanwhile, there are also disadvantages to the PMSM. They are limited speed range, high cost, high stator core loss at high speed, and significant back electromotive force (emf). Instead, spoke-type PMSM is one of the IPMSMs and concentrates

flux by arranging permanent magnets facing each other in the radial direction, allowing a low $(BH)_{max}$ magnet, such as a hexaferrite magnet, to use in the rotor's core [1]. We designed spoke-type PMSM using theoretically developed Mn-based alloys, as shown in Figure 1 [2].

TABLE I Magnetic properties (Magnetic flux density (B_r) , coercivity (H_c) , maximum energy product $((BH)_{max})$, and Curie temperature (T_C) of commercial and calculated permanent magnets

commercial and calculated permanent magnets.						
Magnet	Grade	$B_{\rm r}$ (kG)	H _c (kOe)	$(BH)_{\rm max}$ (MGOe)	$T_{\rm C}\left({ m K}\right)$	
Commercial						
Nd-Fe-B	NdFe35	12.30	11.18	-	-	
	NMX- G1NH	14.20	13.19	-	-	
Alnico	8B	8.30	1.65	5.50	1,113	
	8H	7.40	1.90	5.50	1,113	
	9	11.20	1.38	10.50	1,113	
La-Co SrM	NMF- 15G	4.90	4.80	5.50	700	
Theoretically developed						
SrM	-	4.86 ~ 2.43	4.86 ~ 2.43	5.90	750	

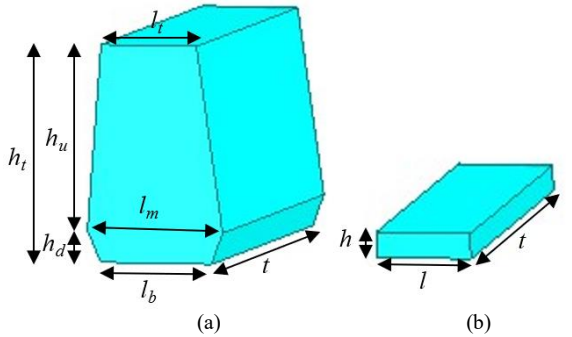


Fig. 2. Two types of magnets for the designed motor: (a) rotor core (RC) magnet and (b) flux directing (FD) magnet.

III. DESIGN OF MAGNETS AND SPECIFICATIONS OF SPOKE-TYPE PMSM

The commercial PMs and theoretically developed magnets are summarized in TABLE I: Nd-Fe-B (NdFe35, G1NH) [3], Alnico (8B, 8H, 9) [4], and La-Co SrM hexaferrite (NMF-15G) [3], and SrM hexaferrite [5]. Figure 2 shows RC and FD magnet designs. The dimensions of the magnets are shown in TABLE II. TABLE III details the specifications of the designed motor for motor performance simulations.

Thus, designed motors were characterized for their motor performance by solving Maxwell's equations with the ANSYS Maxwell software. The designed spoke-type PMSM has 6 phases, 8 poles, 48 slots, and 11 winding turns. A battery voltage of 750 V, a maximum current of 177 A_{rms}, and a peak current density of 20 A_{rms}/mm² were used in the PMSM performance simulations. The spacevector pulse-width modulation (SV-PWM) was used to toggle the switch.

TABLE II

Dimension of r	otor core (RC) and	flux directing (FD) magnets.
	l_{t}	18.6
	$l_{ m m}$	26.37
	I_{b}	21.58
RC (mm)	$h_{ m u}$	34.25
	$h_{ m d}$	5.75
	$h_{ m t}$	40
	t	50.80
	l	15
FD (mm)	h	4
	t	50.80

TABLE III Design specifications of 6-phase spoke-type PMSM

Parameters	Values
Stator outer/inner radius [mm]	134.5 / 80.4
Rotor outer/inner radius [mm]	80 / 24.1785
Stack length [mm]	50.8
Number of poles/slots	8 / 48
Stator turns per coil	11
Rotor/Stator materials soft magnet	M17-29G

IV. MOTOR PERFORMANCE SIMULATION

Figure 3 (a) shows the workflow for the motor performance simulation process, and 2D boundary conditions are shown in Figure 3(b). First, the rotor and stator meshes are generated separately, as shown in the inset on the top left of Figure 3 (a). Then, each mesh with connected nodes can be solved using a finite element (FE) equation for the ferromagnetic core area, permanent magnet area, stator conductor area, and stator circuit. Then, the FE adopted the time discretization for each area and stator circuit. The FE with time discretization linearizes the nonlinear equations, such as the B-H curve of the ferromagnetic core and PM, using Newton Raphson's method. The linearized FEs for each area and stator circuit are assembled into the global matrix and solved with three boundary conditions, which are Dirichlet ($A|_{\overline{AEC}}$ = $A|_{\overline{BFD}} = 0$), Neumann ($\frac{\partial A}{\partial n} = 0$), and periodical ($A|_{\overline{AB}} = 0$) $-A|_{\overline{CD}}$) boundary conditions. From the solved results, the motor performance, such as power, back-EMF, base and maximum speeds, and efficiency, is evaluated by postprocessing. The torque is calculated by Maxwell's stress

$$T = L \int_{\Gamma} (r \times \sigma) \, d\Gamma \tag{1}$$

T =
$$L \int_{\Gamma} (r \times \sigma) d\Gamma$$
 (1)

$$\sigma = \frac{1}{\mu_0} (B \cdot \hat{n}) B - \frac{1}{2\mu_0} (B^2 \hat{n})$$
 (2)

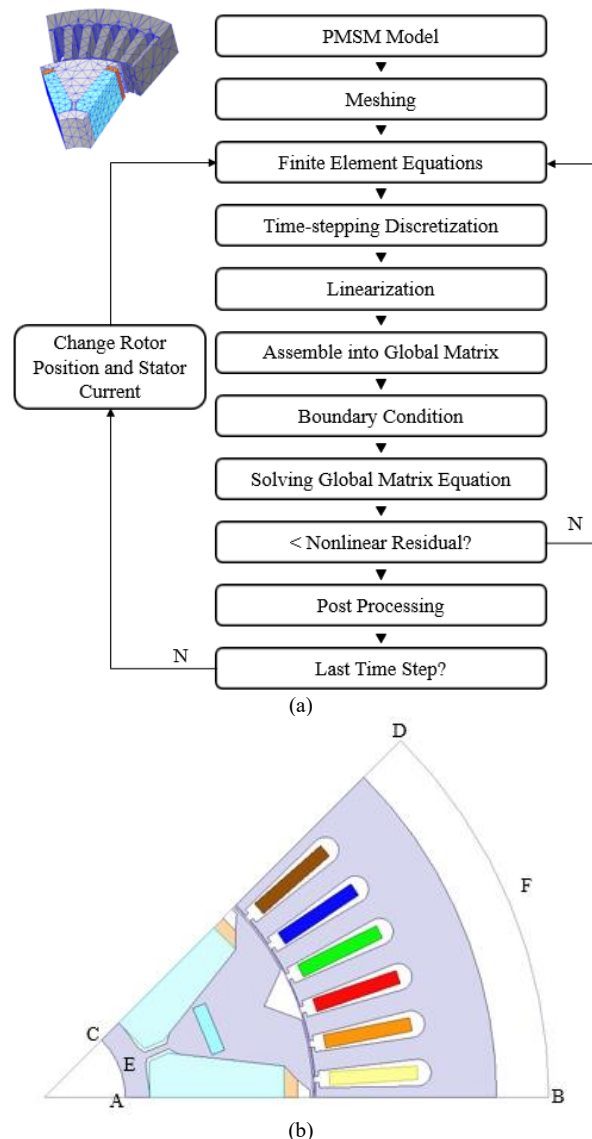


Fig. 3. (a) Workflow for motor performance evaluation and (b) 2D motor for boundary conditions.

$$T_{em} = \frac{2plr^2}{\mu_0} \sum_{k=1}^{N_e} \int_{\theta_k}^{\theta_{k+1}} B_{kr} B_{k\theta} d\theta, \qquad (3)$$

where $B_{kr} = B_{kx} \cos \theta + B_{ky} \sin \theta$, $B_{k\theta} = B_{ky} \cos \theta - B_{ky} \cos \theta$ $B_{kx} \sin \theta$, and $B_{kr \text{ or } k\theta}$ is radial or tangential air-gap flux density. The back-EMF can be calculated by

$$e = \frac{lN}{s} \iint_{S} \frac{\partial A}{\partial t} ds \tag{4}$$

where l is the axial length, N is the number of turns, S is the cross-sectional area, and $\Omega_{+/-}$ is the in/out conductor. To obtain the output power and efficiency, the power loss $(P_{\rm loss})$ should be considered, which is the copper loss $(P_{\rm R} = \frac{3}{2} R_s (i_d^2 + i_q^2))$, eddy current loss $(P_{\rm e} = k_e \omega^2 B^2)$, and hysteresis loss $(P_{\rm h} = k_h \omega B^2)$.

$$P_{loss} = P_R + P_e + P_h = \frac{3}{2} R_s (i_d^2 + i_q^2) + k_h \omega_e^2 B^n + k_e \omega_e B^2,$$
 (6)

$$P_{out} = P_{in} - P_{loss} = 3VI - \frac{3}{2}R_s(i_d^2 + i_q^2) + k_h\omega_e^2B^n + k_e\omega_eB^2,$$
and
(7)

$$Efficiency = \frac{P_{out}}{P_{in}} = \frac{3VI - \left(\frac{3}{2}R_s(i_d^2 + i_q^2) + k_h\omega_e^2B^n + k_e\omega_eB^2\right)}{3VI}. (8)$$

Commercial PM motor performance.						
Magnet	Grade	Torque (Nm)	Toque ripple (%)	Peak power (kW)	Efficiency (%)	
Nd-Fe-B	NdFe35	253	15	297	97	
	NMX- G1NH	290	15	345	97	
	8B	125	22	111	96	
Alnico	8H	138	20	125	96	
	9	125	22	110	96	
SrM	NMF- 15G	189	8	177	96	

V. RESULTS AND DISCUSSION

A. Spoke-type PMSM performance

RE Nd-Fe-B and hexaferrite permanent magnets were used: NdFe35 of the ANSYS Maxwell library and NMX-G1NH (hexaferrite magnet) of Hitachi Metals [3]. Magnetic properties of commercial RE-free Alnico, hexaferrite (La/Co-SrM), and theoretically developed SrM (SrFe₁₂O₁₉) magnets are summarized in TABLE I.

Three kinds of RE-free Alnico (8B, 8H, 9) [4] were used in the PMSM design. Alnico 8B and 8H have the same (BH)_{max} of 5.5 MGOe but different remanent magnetic flux density (B_r) and coercivity (H_c) . Alnico 9 has a higher $(BH)_{\text{max}}$ of 10.5 MGOe but a lower H_c than the Alnico 8 series.

The resulting motor performance with commercial PMs is summarized in TABLE IV. The NMX-G1NH magnet motor outperforms other permanent magnet motors except for the torque ripple in TABLE IV and the maximum speed in Figure 4 (a). It is noted that the torque slowly decreases for the NMX-G1NH motor as the motor speed increases. On the other hand, the NMF-15G hexaferrite motor shows that its torque sharply decreases beyond the base speed, as shown in Figure 4 (b). But its smaller torque ripple and higher maximum speed than the Nd-Fe-B motor are attributed to the saturation of the M17-29G soft magnet by the high B_r and H_c of the Nd-Fe-B hard magnet of the rotor. It was found in this study that even though Alnico 9 holds a higher (BH)_{max} of 10.50 MGOe than Alnico 8H/8B and SrM hexaferrite, its motor performance is not better than the lower $(BH)_{max}$ PMSM. It is noticed that as the H_c/B_r ratio approaches about one, the motor performance gets better. Therefore, this study focuses on the effects of the H_c/B_r ratio on spoke-type PMSM performance. Our theoretically designed SrM (SrFe₁₂O₁₉) hexaferrite magnets were used in the motor

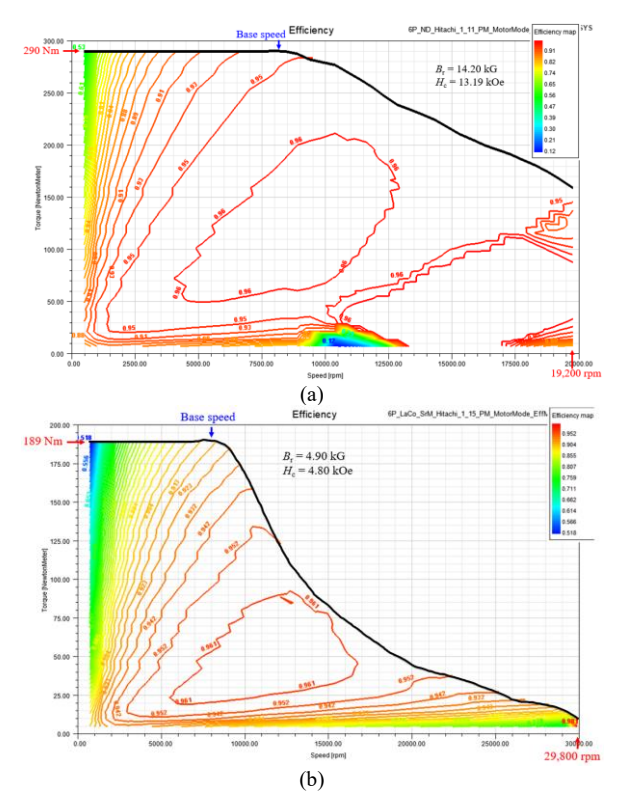


Fig. 4. Efficiency map for (a) commercial Nd-Fe-B (NMX-G1NH: $H_{c}/B_{r} \approx 1$) and (b) commercial SrM hexaferrite (NMF-15G: $H_{c}/B_{r} \approx 1$).

performance simulation. The performance results are reported in Section V.B.

We have found that H_c is more effective than B_r in determining motor performance. For instance, commercial RE-free Alnico 9 holds a 10.5 MGOe of $(BH)_{\rm max}$, an 11.2 kG of B_r , and a 1.38 kOe of H_c . RE-free Alnico 8B and 8H, and hexaferrite show the same $(BH)_{\rm max}$ of 5.5 MGOe in TABLE I. As mentioned above, even though Alnico 9 has much higher B_r , therefore, higher $(BH)_{\rm max}$, Alnico 9 motor performance is worse than Alnico 8B $(H_c = 1.65 \text{ kOe})/8\text{H}$ $(H_c = 1.90 \text{ kOe})$ and hexaferrite $(H_c = 4.80 \text{ kOe})$ permanent magnet motors, as shown in TABLE IV. This is attributed to a lower H_c (Alnico 9) than the other Alnico 8B and 8H and hexaferrite magnets. The commercial hexaferrite permanent magnet (NMF-15G) synchronous motor shows

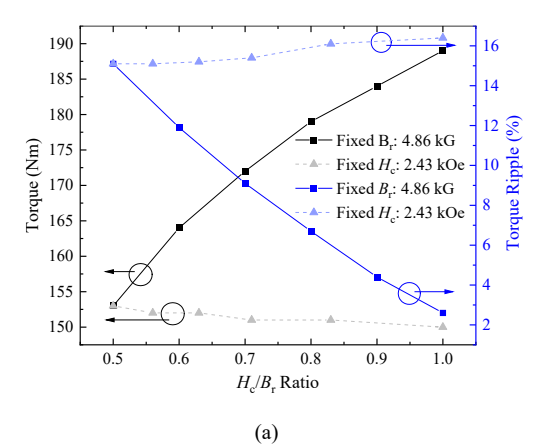
TABLE V Effects of the H_c/B_r ratio at a 4.86 kG of B_r on spoke-type RE-free SrM (SrFe₁₂O₁₉) magnet motor performance.

mi (eii eizeig) magnet meter perfermance.							
$H_{\rm c}/B_{ m r}$	0.5	0.6	0.7	0.8	0.9	1	
$B_{\rm r}({ m kG})$	4.86	4.86	4.86	4.86	4.86	4.86	
H_c (kOe)	2.43	2.92	3.40	3.89	4.37	4.86	
Torque (Nm)	153	164	172	179	184	189	
Toque Ripple (%)	15.1	11.9	9.1	6.7	4.4	2.6	
Peak power (kW)	138	146	155	166	171	178	
Efficiency (%)	96	96	96	96	96	96	

TABLE VI Effects of the H_c/B_t ratio at a 2.43 kOe of H_c on spoke-type SrM (SrFe₁₂O₁₉) magnet motor performance.

$H_{\rm c}/B_{ m r}$	0.5	0.56	0.63	0.71	0.83	1
$B_{\rm r}({ m kG})$	4.86	4.37	3.89	3.40	2.92	2.43
H_c (kOe)	2.43	2.43	2.43	2.43	2.43	2.43
Torque (Nm)	153	152	152	151	151	150
Toque Ripple (%)	15.1	15.1	15.2	15.4	16.1	16.4
Peak power (kW)	138	138	139	140	139	138
Efficiency (%)	96	96	96	96	96	96

the best performance among RE-free magnet motors, as shown in TABLE IV. Therefore, the effects of H_c/B_r ratio of theoretically developed hexaferrite (SrM) permanent magnet in TABLE I on motor performance were investigated in the following section.



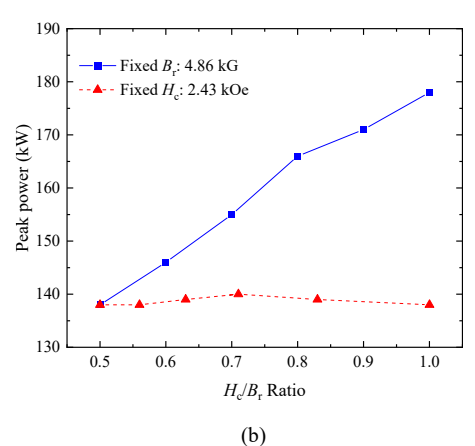


Fig. 5. (a) Torque and torque ripple and (b) peak power for theoretically designed SrM ferrite motor

B. RE-free SrM hexaferrite motor performance with various H_c/B_r ratios

The magnetic properties of theoretically developed SrM (SrFe₁₂O₁₉) hexaferrite [5] in TABLE I were used in

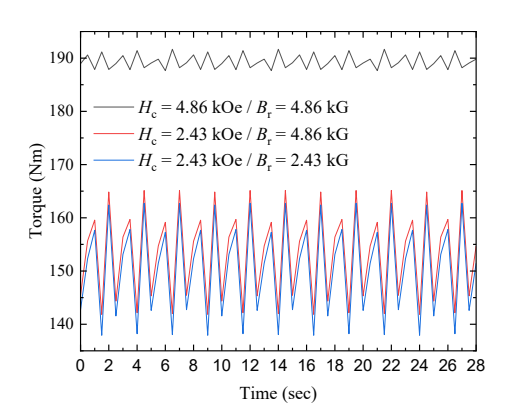


Fig. 6. Output torque of spoke-type PMSM at the base speed.

the spoke-type PMSM performance simulation, therefore, investigating the effects of $H_{\circ}/B_{\rm r}$ ratio on motor performance. The simulated motor performance results are summarized in TABLE V with a fixed $B_{\rm r}$ and TABLE VI with a fixed $H_{\rm c}$.

Figure 5 shows the effects of H_c/B_r ratio ≤ 1 on motor performance. The torque and peak power at a 4.86 kG of B_r increase remarkably to 189 Nm and 178 kW from 153 Nm and 138 kW, respectively, as H_c increases to 4.86 kOe from 2.43 kOe, but the torque ripple significantly decreases to 2.6 % from 15.1 %. It is worth noting that even though B_r is lower, H_c can help improve motor performance. As a result, the motor performs best when the H_c/B_r ratio approaches one.

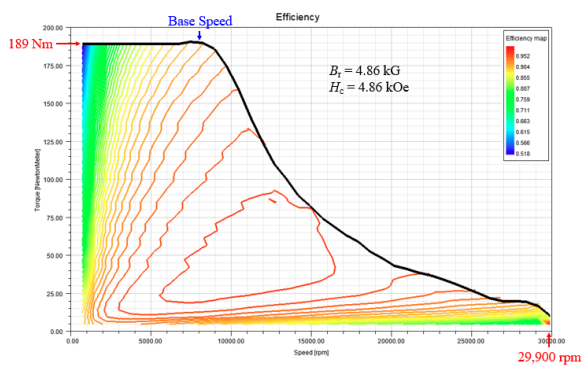
On the other hand, when H_c is fixed at 2.48 kOe, the torque, torque ripple, and peak power are unnoticeably changed with the H_c/B_r ratio, as shown in Figure 5. It is found that regardless of $(BH)_{\rm max}$, the coercivity (H_c) plays a dominant role in motor performance.

To investigate the effects of the H_c on SrM (SrFe₁₂O₁₉) hexaferrite PMSM performance, the output torque was studied at the base speed. When the H_c changes to 2.43 kOe from 4.86 kOe at a fixed 4.86 kOe of B_r , the torque dramatically lowers to 150 Nm from 189 Nm, and the torque ripple increases, as shown in Fig. 6. It is noteworthy that the torque and torque nipple are unnoticeably changed even though the B_r increases to 4.86 kOe from 2.43 kOe at a fixed 2.43 kOe of H_c . Thus, the H_c has more effective role than B_r of permanent magnet in PMSM performance.

Finally, we studied the hexaferrite PMSM efficiency when the H_c/B_r ratio equals one. Fig. 7 shows hexaferrite PMSM efficiency map with the two different H_c/B_r ratios which are 4.68 kOe (H_c)/4.68 kOe (B_r) and 2.43 kOe (H_c)/2.43 kOe (B_r). The ratio of 2.44/2.43 kOe decreases the torque to 189 Nm from 290 Nm ($H_c/B_r = 4.86$ kOe/4.86 kOe), but increases the maximum speed to about 72,000 rpm from 30,000 rpm (Hc/Br = 4.86 kOe/4.86 kOe).

VI. CONCLUSIONS

Spoke-type PMSMs were designed and characterized for their motor performance. Even though a magnet



possesses a high $(BH)_{\rm max}$, coercivity has a more influential role than remanent magnetization in motor performance. It

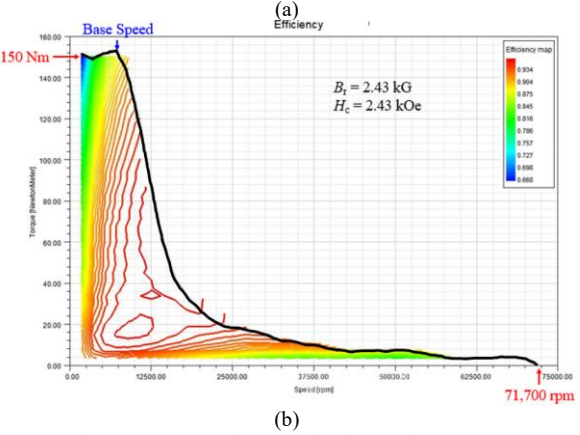


Fig. 7. Efficiency map for theoretically designed SrM hexaferrite PMSM with the ratio of 1; (a) $(H_c = 4.86 \text{ kOe} / B_r = 4.86 \text{ kG})$ and (b) $(H_c = 2.43 \text{ kOe} / B_r = 2.43 \text{ kG})$.

was confirmed by Alnico PMSM motor performance. Even though commercial RE-free Alnico 9 holds a 10.5 MGOe of $(BH)_{\rm max}$ and an 11.2 kG of $B_{\rm r}$, which are higher than those of Alnico 8B/8H and SrM hexaferrite permanent magnets, the Alnico 9 PMSM shows poorer motor performance than the others. This is attributed to a lower 1.38 kOe of $H_{\rm c}$ than Alnico 8B/8H and SrM hexaferrite. Furthermore, Alnico 8B/8H and SrM hexaferrite magnets have the same $(BH)_{\rm max}$ of 5.5 MGOe, but the SrM hexaferrite motor outperforms the Alnico motors. It was found that the coercivity of the magnet is a crucial role in determining PMSM performance.

ACKNOWLEDGMENT

This work was in part supported by the National Science Foundation (NSF) IUCRC under Grant No. 1650564.

REFERENCES

- [1] Min-Jae Jeong, Kang-Been Lee, Hyun-Jo Pyo, Dong-Woo Nam, and Won-Ho Kim, "A Study on the Shape of the Rotor to Improve the Performance of the Spoke-Type Permanent Magnet Synchronous Motor," *Energies*, vol. 14(13), 3758 (2021).
- [2] Hoyun Won, Yang-Ki Hong, Woncheol Lee, Minyeong Choi, Shuhui Li, and Hwan-Sik Yoon, "Low Torque Ripple Spoke-type Rare-Earth Free Permanent Magnet Motor for

- Electric Vehicle," 2019 IEEE International Electric Machines & Drives Conference, San Diego, CA, May 12-15, (2019).
- [3] Hitachi Metals: https://www.hitachi-metals.co.jp/e/
- [4] Arnold: https://www.arnoldmagnetics.com/wp-content/uploads/2017/10/Cast-Alnico-Permanent-Magnet-Brochure-101117-1.pdf
- [5] Jihoon Park, Yang-Ki Hong, Seong-Gon Kim, Sungho Kim, Laalitha S.I. Liyanage, Jaejin Lee, Woncheol Lee, Gavin S. Abo, Kang-Heon Hur, and Sung-Yong An, "Maximum energy product at elevated temperatures for hexagonal strontium ferrite (SrFe₁₂O₁₉) magnet," *Journal of Magnetism and Magnetic Materials*, vol. 355, pp. 1-6 (2014).